

Search for New Particles with Flying Quantum Sensors in Space

Xingming Huang,^{1,2,3, a)} Yuanhong Wang,^{1,2,3, a)} Min Jiang,^{1,2, b)} Xiang Kang,^{1,2,3} Haowen Su,^{1,2} Zehao Wang,^{1,2} Qing Lin,^{4,5} Wenqiang Zheng,⁶ Yuan Sun,⁷ Liang Liu,⁷ Xinhua Peng,^{1,2,3, c)} Zhengguo Zhao,^{4,5} and Jiangfeng Du^{1,2,3,8}

¹⁾CAS Key Laboratory of Microscale Magnetic Resonance and School of Physical Sciences, University of Science and Technology of China, Hefei, Anhui 230026, China

²⁾CAS Center for Excellence in Quantum Information and Quantum Physics, University of Science and Technology of China, Hefei, Anhui 230026, China

³⁾Hefei National Laboratory, University of Science and Technology of China, Hefei 230088, China

⁴⁾State Key Laboratory of Particle Detection and Electronics, University of Science and Technology of China, Hefei 230026, China

⁵⁾Deep Space Exploration Laboratory/Department of Modern Physics, University of Science and Technology of China, Hefei 230026, China

⁶⁾Zhejiang Provincial Key Laboratory and Collaborative Innovation Center for Quantum Precision Measurement, College of Science, Zhejiang University of Technology, Hangzhou 310023, China

⁷⁾Key Laboratory of Quantum Optics, Shanghai Institute of Optics and Fine Mechanics, Chinese Academy of Sciences, Shanghai 201800, China

⁸⁾Institute of Quantum Sensing and School of Physics, Zhejiang University, Hangzhou 310027, China

(Dated: 22 October 2024)

Recent advancements in space science and technologies offer exciting prospects for investigating novel research that is unattainable within terrestrial laboratories. Here we propose the implementation of space-based quantum sensing to explore ultralight new particles beyond the standard model. The central idea involves probing long-range interactions between spin ensembles of space quantum sensors and the particles residing within Earth, mediated by ultralight particles. We show that such interactions can be substantially enhanced in space platforms and thus increase the search sensitivity. In contrast to their terrestrial counterparts, space-based quantum searches exhibit remarkable velocity enhancements, approaching the first cosmic speed, and thus enables the exploration of unexplored parameter space concerning ultralight new particles. Furthermore, the substantial abundance of electrons and nucleons within Earth plays a crucial role in extending the scope of our mission. Our projected search sensitivity can surpass the sensitivities of both terrestrial experiments and proposals by up to approximately 7 orders of magnitude. We also briefly discuss other space mission, including “space-ground integrated” network of quantum sensors for dark matter searches.

Numerous experiments have been conducted in particle accelerators to search for microscopic particles. These experiments involve the microscopic-level interactions of particles¹. However, these methods are inadequate when it comes to searching for ultralight exotic particles, which are predicted by various theories beyond the standard model. Some examples of these exotic particles include axions and axion-like particles^{2,3}, dark photons⁴, paraxions⁵, familons⁶, and majorons⁷. These hypothetical particles could be candidates for dark matter particles^{8,9}, and their discovery could provide crucial insights into fundamental physics, such as the solution to the strong charge-parity problem^{2,10} and the study of cosmic microwave background anisotropies¹¹. They are predicted to act as force mediators, enabling their detection through macroscopic interactions between standard-model particles¹²⁻¹⁴. Such exotic interactions possess significant long force ranges due to that their force mediators are ultralight, allowing for interactions over distances of hundreds of kilometers between standard-model particles. Various terrestrial experiments with atoms and molecules have been conducted at the macroscopic level to search for ul-

tralight exotic particles. These experiments utilize optical magnetometers¹⁵⁻¹⁷, spin-based amplifiers¹⁸⁻²⁵, atomic comagnetometers²⁶⁻³⁰, nitrogen-vacancy diamonds^{31,32}, torsion pendulums³³⁻³⁵, and trapped ions^{36,37}, etc.

Despite numerous terrestrial experiments aimed at exploring exotic particles, no exotic particles beyond the standard model have been detected. This outcome can be primarily attributed to two significant challenges. First, the amplitudes of the macroscopic interactions are limited by the achievable velocity of terrestrial experiments. To effectively search for new particles through velocity-dependent macroscopic interactions, it is prerequisite to accelerate macroscopic objects (e.g., an ensemble of fermions) to high velocities. However, current terrestrial searches suffer from relatively small velocities of macroscopic objects, typically ranging below 20 m/s [15,16,20]. Even with potential future advancements, the achievable velocity of macroscopic objects in terrestrial experiments still falls significantly below the first cosmic speed. Second, the small number of interacting standard-model particles also limits the amplitudes of macroscopic interactions. For example, the number of polarized electrons in current laboratory setup is less than 10^{25} [16]. One major obstacle lies in the fact that as the mass of macroscopic objects increases, the task of accelerating and maintaining them at high velocities in laboratories becomes increasingly difficult. Therefore, it is imperative to develop novel methods in searches for exotic particles, which could provide a new

^{a)}These authors contributed equally to this work

^{b)}dxjm@ustc.edu.cn

^{c)}xhpeng@ustc.edu.cn

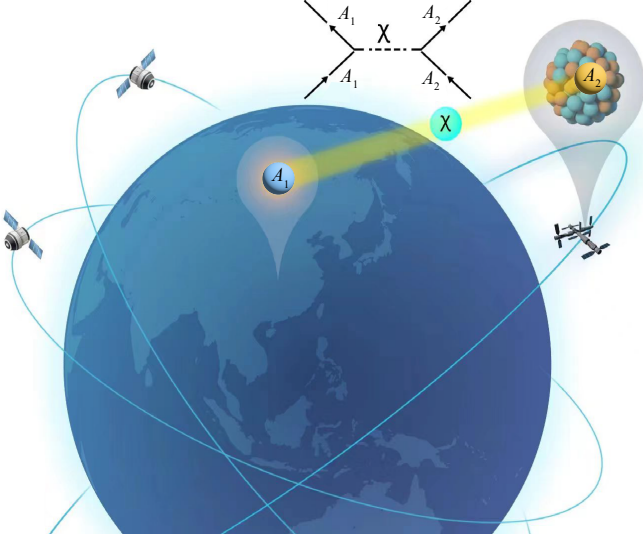


FIG. 1. Concept of space-based searches for ultralight exotic particles. The search strategy involves equipping highly-sensitive quantum spin sensors on space platforms to leverage their relative motion with Earth. Mediated by ultralight exotic particles χ , a class of new long-range spin-dependent interactions can be generated between the standard-model particle A_1 within the Earth and the spin-particle A_2 in space platform, even over vast distances spanning hundreds of kilometers. Due to the high relative motion close to the first cosmic speed between space-based spin sensors and Earth, a large class of long-range interactions can be greatly enhanced compared with terrestrial experiments and produce enhanced pseudomagnetic fields on the spin sensors.

source for parity symmetry violation. Careful investigations on those interactions may give clues for understanding fundamental physical questions like matter-antimatter asymmetry of the Universe.

In this paper, we describe a novel proposal for a space-based quantum sensing aimed at searching for ultralight new particles with an unprecedented level of search sensitivity, surpassing that of terrestrial experiments. Our approach involves deploying spin-based quantum sensors on space platforms to leverage their relative motion with Earth, creating a high-velocity laboratory condition for studying long-range spin-dependent interactions mediated by exotic particles. The velocity of the space quantum sensor could reach 7.67 km/s close to the first cosmic speed and surpass previous experimental velocities by orders of magnitude^{15,16,20}, which provides a unique opportunity to search for exotic particles under unprecedented high-velocity conditions. In addition, the substantial geoelectrons and nucleons within Earth play a critical role in improving the search sensitivity^{28,30}. Our work showcases that the projected search sensitivity for new particles exceeds the achievements of both terrestrial experiments and proposals by up to about 7 orders of magnitude. Furthermore, in addition to searching for new particles via long-range spin-dependent interactions, we also briefly discuss other fundamental physics that can be searched by quantum sensing technique in space. A “space-ground integrated” network

of quantum sensors can be established by connecting space quantum sensors with terrestrial quantum sensors, and used to search for dark matter. Such a network has the potential to significantly enhance sensitivity for various dark matter models by several orders of magnitude^{38–44}.

banerjee2020searching,anderson2020direct1

Long-range spin-dependent interactions

We first discuss the potential for long-range interactions between a spin ensemble within an aerospace vehicle and various particles, including geoelectrons and nucleons, present within Earth. Numerous theories beyond the standard model propose the existence of fifteen distinct types of spin-dependent interactions mediated by new bosons¹³. As depicted in Fig. 1, these ultralight bosons denoted by χ could induce long-range spin-dependent interactions between the particle A_1 within the Earth and the spin-particle A_2 in the aerospace vehicle, even over vast distances spanning hundreds of kilometers. These interactions can be classified into two distinct groups: spin-spin interactions and spin-mass interactions. In this study, we use the interaction formats adopting the numbering scheme in ref. [13]. The investigated spin-dependent interactions are as follow:

$$V_{4+5} = -f_{4+5} \frac{\hbar^2}{8\pi m_1 c} [\hat{\sigma}_2 \cdot (\vec{v} \times \hat{r})] \left(\frac{1}{\lambda r} + \frac{1}{r^2} \right) e^{-r/\lambda}, \quad (1)$$

$$V_{6+7} = -f_{6+7} \frac{\hbar^2}{4\pi m_\mu c} \left(\frac{1}{\lambda r} + \frac{1}{r^2} \right) e^{-r/\lambda} \times [(\hat{\sigma}_1 \cdot \vec{v})(\hat{\sigma}_2 \cdot \hat{r}) + (\hat{\sigma}_1 \cdot \hat{r})(\hat{\sigma}_2 \cdot \vec{v})], \quad (2)$$

$$V_8 = f_8 \frac{\hbar}{4\pi c} (\hat{\sigma}_1 \cdot \vec{v})(\hat{\sigma}_2 \cdot \vec{v}) \left(\frac{1}{r} \right) e^{-r/\lambda}, \quad (3)$$

$$V_{12+13} = f_{12+13} \frac{\hbar}{8\pi} (\hat{\sigma}_2 \cdot \vec{v}) \left(\frac{1}{r} \right) e^{-r/\lambda}, \quad (4)$$

$$V_{14} = f_{14} \frac{\hbar}{4\pi} [(\hat{\sigma}_1 \times \hat{\sigma}_2) \cdot \vec{v}] \left(\frac{1}{r} \right) e^{-r/\lambda}, \quad (5)$$

$$V_{16} = -f_{16} \frac{\hbar^2}{8\pi m_\mu c^2} \left(\frac{1}{r} \right) e^{-r/\lambda} \times \{[\hat{\sigma}_1 \cdot (\vec{v} \times \hat{r})](\hat{\sigma}_2 \cdot \vec{v}) + (\hat{\sigma}_1 \cdot \vec{v})[\hat{\sigma}_2 \cdot (\vec{v} \times \hat{r})]\}, \quad (6)$$

$$V_2 = f_2 \frac{\hbar c}{4\pi} (\hat{\sigma}_1 \cdot \hat{\sigma}_2) \left(\frac{1}{r} \right) e^{-r/\lambda}, \quad (7)$$

$$V_{11} = -f_{11} \frac{\hbar^2}{4\pi m_\mu} [(\hat{\sigma}_1 \times \hat{\sigma}_2) \cdot \hat{r}] \left(\frac{1}{\lambda r} + \frac{1}{r^2} \right) e^{-r/\lambda}, \quad (8)$$

where $\hat{\sigma}_i$ is the Pauli spin-matrix vectors of i th particle A_i and m_i is its mass, m_μ is the reduced mass of m_1 and m_2 , \vec{v} represents the relative velocity between A_1 and A_2 particles, r denotes the distance between them, \hat{r} is the corresponding unit vector, and $\lambda = \hbar/m_\chi c$ denotes the force range, with m_χ being the mass of ultralight exotic particle as force mediator. f_i is the dimensionless coupling strengths of V_i , which could be mediated by the ultralight exotic particles χ , such as axions, Z' bosons, and paraphotons¹⁴.

Long-range spin-dependent interactions can generate pseudomagnetic fields on the spin ensemble in an aerospace vehicle. The spin-dependent interactions can be mathematically

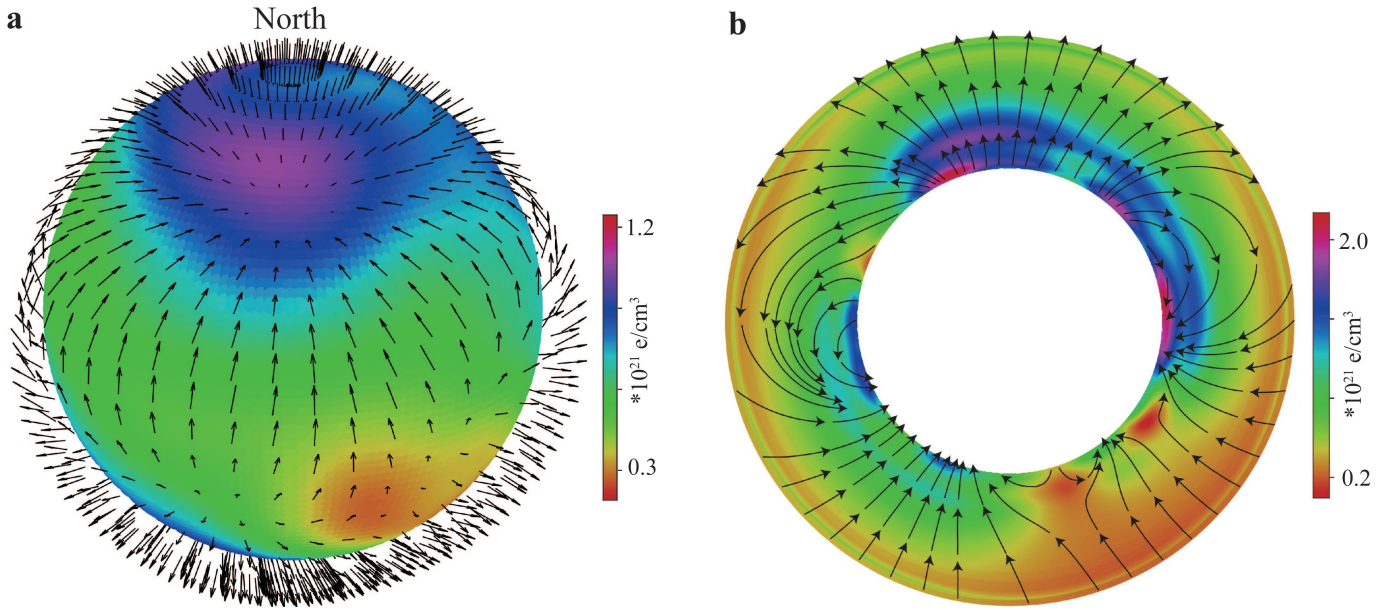


FIG. 2. **Simulation results of polarized geoelectrons distribution.** **a**, The distribution of polarized geoelectrons on the spherical surface at the center of the Earth, with a radius of 5000 km. The black arrows indicate the direction of the geoelectron spins, and the color shading represents the magnitude of the polarized geoelectron-spin density. **b**, The distribution of polarized geoelectrons in the cross section between the orbital plane of the China Space Station and Earth. The representation of black arrows and color shading follows the same conventions as in (a). However, the component of the field perpendicular to the orbital plane of the space station (into or out of the page) is not depicted. Additionally, the geoelectron-spin density within the core (indicated by the white central circle) is assumed to be zero.

expressed as $V_{\text{exotic}} = -\mu_2 \vec{B}_{\text{pseu}} \cdot \hat{\sigma}_2$, which is similar to Zeeman interactions. Here μ_2 denotes the magnetic moment of the spin particle A_2 in the aerospace vehicle. The spin A_2 located on one side of a vertex can experience the pseudomagnetic fields generated by another particle A_1 situated on the other vertex¹⁸. To clearly illustrate the properties of pseudomagnetic fields, we consider three specific examples: spin-spin interactions V_{14} , V_8 , and spin-mass interaction V_{4+5} . The expressions for the pseudomagnetic fields \vec{B}_{14} , \vec{B}_8 and \vec{B}_{4+5} are as follows:

$$\vec{B}_{14} = - \int_V \rho(\vec{r}) \frac{f_{14} \hbar}{4\pi\mu_2} (\hat{\sigma}_1 \times \vec{v}) \left(\frac{1}{r} \right) e^{-r/\lambda} d\vec{r}, \quad (9)$$

$$\vec{B}_8 = - \int_V \rho(\vec{r}) \frac{f_8 \hbar}{4\pi c \mu_2} (\hat{\sigma}_1 \cdot \vec{v}) \left(\frac{\vec{v}}{r} \right) e^{-r/\lambda} d\vec{r}, \quad (10)$$

$$\vec{B}_{4+5} = \int_V \frac{\rho_m(\vec{r}) f_{4+5} \hbar^2}{8\pi m_1 c \mu_2} (\vec{v} \times \hat{r}) \left(\frac{1}{\lambda r} + \frac{1}{r^2} \right) e^{-r/\lambda} d\vec{r}, \quad (11)$$

where V represents the integration volume of the particles A_1 within the Earth, $\rho(\vec{r})$ is the polarized geoelectrons density of particles A_1 at \vec{r} , and $\rho_m(\vec{r})$ is the mass density of nucleon particles A_1 at \vec{r} . Other spin-dependent interactions can give rise to similar pseudomagnetic fields. Notably, enhancing the relative velocity between the particles A_1 and A_2 and increasing the number of A_1 particles are crucial to increase the pseudomagnetic fields of long-range exotic interactions.

Space-based quantum searches

We propose a space-based search strategy that involves equipping space platforms with highly-sensitive spin sensors.

Our aim is to demonstrate a new opportunity for studying long-range spin-dependent interactions mediated by ultralight bosons (see Fig. 1). The pseudomagnetic fields, as described by Eqs. (9)–(11), are directly proportional to the relative velocity and the number of particles. Space platforms provide unparalleled experimental conditions^{43,45–50}, particularly in terms of their high velocities. For example, the International Space Station, the China Space Station, medium Earth orbit satellites, and geostationary satellites exhibit velocities of up to 7.67 km/s, 7.67 km/s, 4.5 km/s, and 3.1 km/s, respectively. Among these platforms, the space station stands out as an excellent choice due to its high velocity, approaching the first cosmic speed and exceeding the velocities achieved in previous terrestrial experiments by a factor of at least 300 [15,16,20]. In addition to these advantages, the Earth possesses an exceptional number of particles, which serve as natural sources of geoelectrons and nucleons. Rather than relying on constrained particles from laboratory sources, we utilize polarized geoelectrons due to their abundant quantity, remarkably improving the available polarized particles by 17 orders of magnitude⁵¹. Furthermore, the Earth's unpolarized nucleons are capable of engaging in long-range spin-dependent interactions, offering a 26 orders-of-magnitude increase in the number of unpolarized particles¹⁵. The combination of space-based quantum sensors and Earth's particle sources should provide a promising avenue for probing long-range interactions.

The China Space Station is completed in 2022 [47] and serves as a suitable platform for performing our space-based search scheme. The relative motion between the China Space

Station and the Earth encompasses the space station's revolution and the Earth's rotation. The motion parameters of the space station are derived from its two-line element (TLE) data⁵². The space station's revolution is described by four parameters: the revolution-orbit radius (R) of 6700 km, the mean motion (n) of 15.61 (representing daily orbital laps of the space station), the orbital inclination (θ) of 41.45 degrees (representing the angle between the revolution plane of the space station and the equatorial plane of the Earth), and the right ascension of the ascending node (ϕ) of 84.98 degrees (representing the relative position of the space station's orbit in Earth-Centered Inertial coordinate). The Earth's rotation has a period of 24 hours, with the rotation axis directed from the South Pole to the North Pole. By combining the space station's revolution with the Earth's rotation, we can determine the conditions for the high-velocity experiments.

The data concerning the distribution of polarized geoelectron-spin density plays a crucial role in estimating the pseudomagnetic fields of long-range spin-dependent interactions. The polarized geoelectrons originate from the inverse polarization of unpaired geoelectrons within the geomagnetic field²⁸. The polarized geoelectron-spin density can be determined using the following equation:

$$\rho(\vec{r}) = \rho_e(\vec{r}) \frac{2\mu_B B_e(\vec{r})}{k_B T(\vec{r})}, \quad (12)$$

where μ_B represents the Bohr magneton, k_B denotes Boltzmann's constant, $T(\vec{r})$ is the temperature at location \vec{r} , and $\rho_e(\vec{r})$ represents the density of "equivalent $\text{Fe}^{2+} e^-$ " at \vec{r} , which can be obtained from various fields such as deep-Earth mineral physics, geochemistry, and seismology²⁸. The geomagnetic field $B_e(\vec{r})$ is derived from a magnetic potential approximated by a 12th-order associated Legendre expansion in the World Magnetic Model^{53,54}. The average polarization of geoelectrons is about 10^{-7} [28]. By employing the three input parameters, $T(\vec{r})$, $\rho_e(\vec{r})$, and $B_e(\vec{r})$, the distribution of polarized geoelectron-spin density can be determined from numerical simulations. Figure 2a shows the overall characteristics of the polarized geoelectrons distribution, which is characterized by a significant degree of non-uniformity. In Fig. 2b, we show the distribution of polarized geoelectrons in the cross section between the orbital plane of the China Space Station and Earth. The polarization of geoelectrons varies across different locations within the plane. The white circular area signifies that the unpaired geoelectrons within the Earth's core do not contribute to polarized spins due to the high temperature of the core, which can reach up to 5400 K [55]. In our simulation, we divide the Earth into 4 million sections, calculate and then aggregate the pseudomagnetic magnetic fields generated by polarized geoelectrons in each section. The total number of polarized geoelectrons in simulation surpasses 10^{42} .

We further use numerical simulation to analyze the properties of pseudomagnetic fields, including their orientations, amplitudes, and frequency spectra. We take B_{14} , B_8 , and B_{4+5} as examples, and other pseudomagnetic signals not shown are also analyzed. Figure 3 demonstrates the distinct characteristics of these pseudomagnetic fields on the orbit of the China Space Station. For instance, B_{14} primarily exhibits a direction

perpendicular to the orbit plane (Fig. 3a1), with its amplitude oscillating periodically. As a consequence, in order to maximize the signal from B_{14} , it is essential to align the sensitive axes of quantum sensors perpendicular to the orbit plane. This arrangement allows for the largest projection of B_{14} . For the B_8 pseudomagnetic field, its main direction aligns with the orbital velocity vector of the space station (Fig. 3b1). The sensitive directions of quantum sensors are required to follow the space station's velocity vector. Fortunately, because one side of the China Space Station continuously maintains facing the Earth for communication purposes, the sensitive directions of quantum sensors can be adjusted automatically along the velocity vector without the necessity of time-dependent adjustments. In the case of B_{4+5} , the dominant component is perpendicular to the orbit plane due to $\vec{B}_{4+5} \propto \vec{v} \times \hat{r}$ according to Eq. (11). The dominant component, albeit challenging to quantify, remains constant throughout. Fortunately, the rotation of the Earth imparts a velocity to the space station that deviates from the orbital plane. Consequently, a pseudomagnetic field is present within the orbit plane (Fig. 3c1), which can be further modulated by the rotation of the space station. Consequently, in order to measure B_{4+5} with high sensitivity, it is necessary to align the sensitive axes of quantum sensors along the orbital radial direction.

With the terrestrial constraints on the coupling constants f_{14} , f_8 , f_{4+5} [29,30], the simulations calculate the values of B_{14} , B_8 , and B_{4+5} (Fig. 3a2, b2, and c2) in the optimal detection directions discussed above. Their oscillating amplitudes surpass 200 pT, 20 pT, and 1.5 fT, respectively, holding promising potential for detection with existing spin sensors^{8,56}. Fourier transformation is performed on the simulated data to analyze their oscillation frequencies. As shown in Fig. 3a3, b3, and c3, the primary frequencies correspond to the space-station revolution at $df_1 \approx 0.189$ mHz. While B_{4+5} exhibits a single-frequency oscillation, the spectra for B_{14} and B_8 display multiple peaks. This is attributed to the association of B_{14} and B_8 with the orientation of polarized geoelectron spins. Consequently, the Earth's rotation that occurs at ≈ 0.012 mHz leads to the splitting of the main peak with a frequency difference of $df_2 \approx 0.012$ mHz. As shown in Fig. 2a, b, the distribution of polarized geoelectron spins within the Earth is asymmetric and gives rise to weaker high-frequency harmonic peaks in Fig. 3a3, b3. In contrast, B_{4+5} is linked to spherically symmetrical unpolarized nucleons within the Earth, resulting in an oscillation frequency equal to the frequency of space-station revolution. These distinct spectral features provide unique ways to confidently discern exotic signals of long-range spin-dependent interactions from sources of noise.

Space quantum sensors as particle detectors

Nuclear spin sensors possess exceptional energy resolution, making them highly promising for detecting the pseudomagnetic fields. In this proposal, we suggest employing a nuclear spin-based amplifier for the searches of ultralight particles. The key element of this sensor involves the spatial overlapping of noble gas and alkali-metal gas within a single vapor cell, such as ^{129}Xe -Rb system and ^3He -K sys-

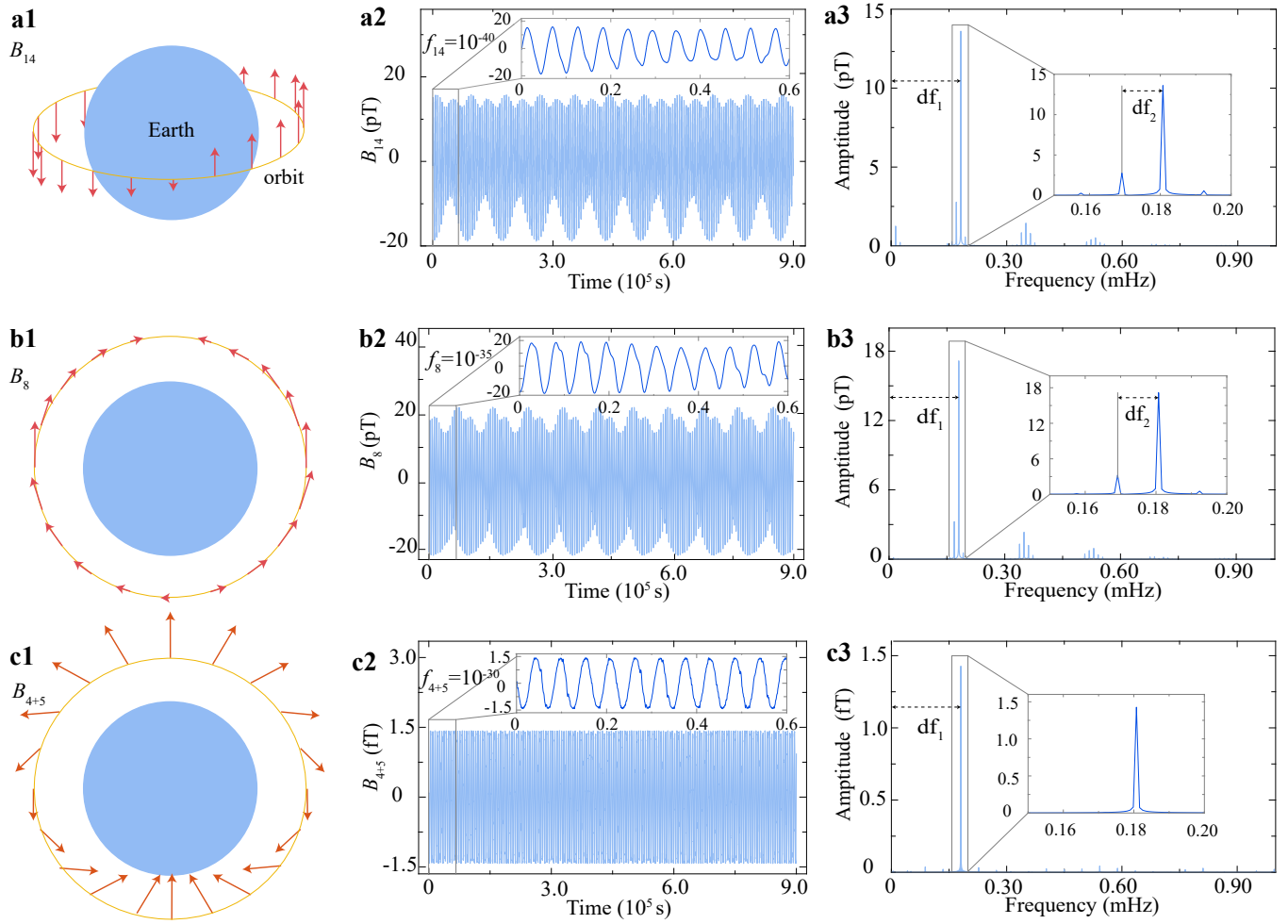


FIG. 3. Results of the simulated pseudomagnetic signals on the orbit of the China Space Station. **a1**, **b1**, and **c1** show the orientations for the oscillating components of B_{14} , B_8 , and B_{4+5} in various locations of the orbit of the China Space Station (see text for the details). **a2**, **b2**, and **c2** show the temporal variation of the simulated signals of B_{14} , B_8 , and B_{4+5} on the orbit. These signals are the projections of the pseudomagnetic fields in the optimal detection directions discussed above. The absolute magnitude of their amplitudes is based on assuming that the coupling constants f_{14} , f_8 , f_{4+5} are consistent with the terrestrial constraints^{29,30}. **a3**, **b3**, and **c3** are the frequency spectra for B_{14} , B_8 , and B_{4+5} , respectively. Their primary frequencies correspond to the space-station revolution at $df_1 \approx 0.189$ mHz. The spectra for B_{14} and B_8 display multiple peaks due to their association with the orientation of polarized geoelectron spins. The split of main peak with a frequency difference of $df_2 \approx 0.012$ mHz is generated by the rotation of the Earth. Moreover, the asymmetry of polarized geoelectron-spin distribution gives rise to their weaker high-frequency harmonic peaks. In contrast, B_{4+5} is linked to spherically symmetrical unpolarized nucleons within the Earth, resulting in an oscillation frequency equal to the frequency of space-station revolution.

tem. Based on the spin-exchange collisions, the nuclear spins of the noble gas are hyperpolarized by the optically pumped alkali-metal gas As demonstrated in ref. [8], these hyperpolarized nuclear spins then serve as pre-amplifiers for the pseudomagnetic signals, which are subsequently detected by the alkali-metal spins. The amplification factor exceeds 100 [8]. Because of the substantial magnetic quantum amplification effect of the spin-based amplifier, its experimentally observed sensitivity surpasses $100 \text{ fT/Hz}^{1/2}$. A series of terrestrial experiments, which are referred as ‘‘Spin Amplifier for Particle PHysics REsearch (SAPPHIRE)’’ project, use spin-based amplifiers to search for new physics and place new constraints on exotic particles^{8,18–20}. This approach offers a powerful method for investigating the signals in

our proposed scheme. The spin-based amplifier operates at near ambient temperature and atmospheric pressure, making it suitable for achieving miniaturization in space-based quantum sensing. In addition to nuclear spin-based amplifier, other nuclear spin sensors, such as dual-species nuclear-spin comagnetometers^{57–59} and self-compensating noble-gas-alkali-metal comagnetometers²⁶, can also serve as sensitive sensors for probing these pseudomagnetic signals.

To ensure optimal performance of spin sensors in space station, several issues that differ from typical conditions encountered on the ground must be taken into account. First, the environmental geomagnetic field varies periodically by about $20 \mu\text{T}$ due to the motion of space station. To suppress this magnetic noise, we can use the fluxgate magne-

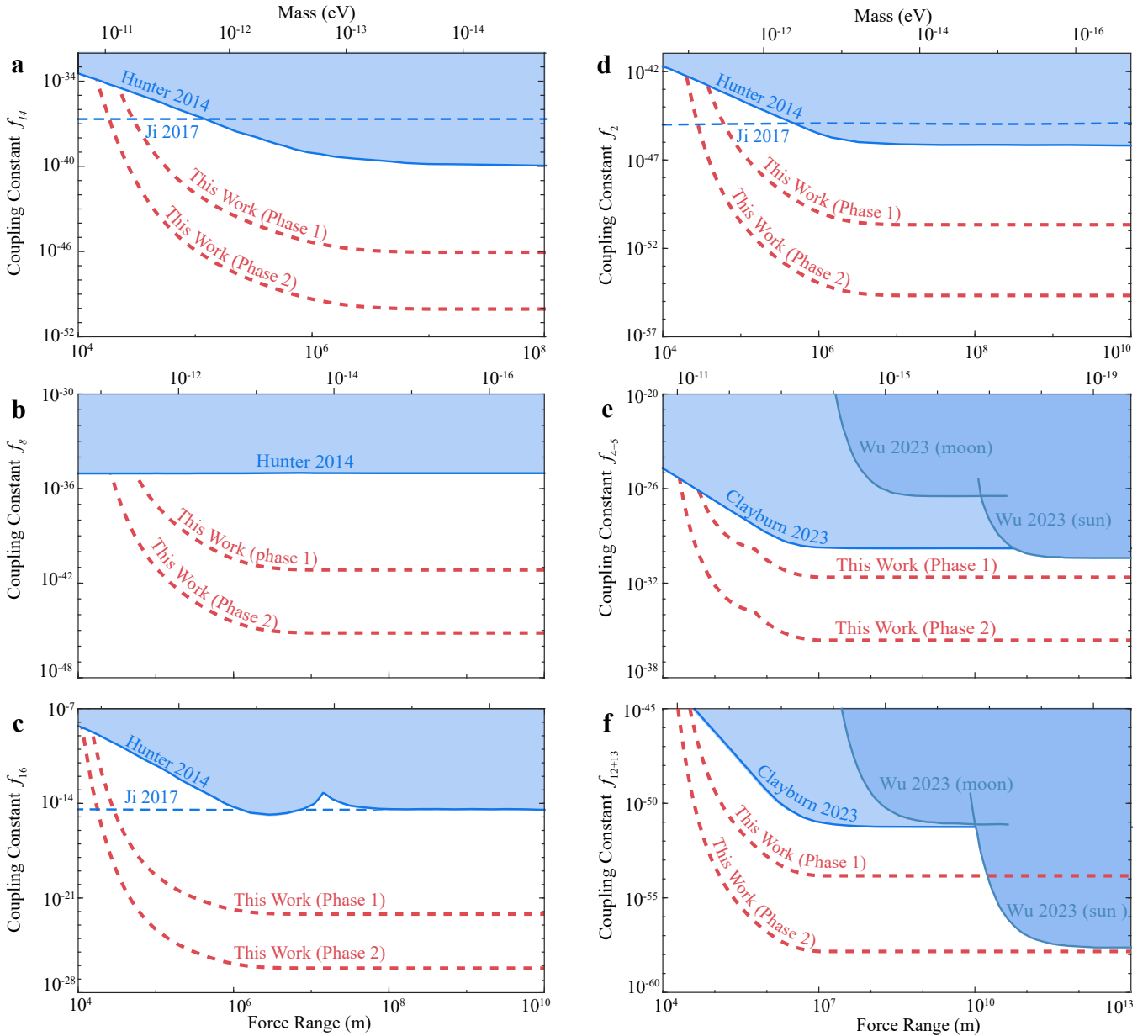


FIG. 4. **Space-based search sensitivity for long-range spin-dependent interactions.** For the the coupling constants of spin-spin interactions, the most stringent limits for the force range $\lambda > 10^4$ m are set by the polarized geoelectrons experiment²⁹ and the proposed high-density SmCo₅ Source experiment¹⁶. Their constraints and sensitivities are depicted with blue solid and dotted lines. For the coupling constants of spin-mass interactions, the most stringent limits for the force range $\lambda > 10^{11}$ m are set by Wu *et al.*²⁷. Their work utilizes the Sun and the Moon as mass sources and Earth rotation as modulation. For the force range $10^4 \text{ m} < \lambda < 10^{10}$ m, the most stringent limits are set by Clayburn *et al.*³⁰, utilizing the Earth as mass sources. Both of the constraints are depicted with the blue solid lines. **a**, **b**, **c**, **d**, **e**, and **f** show the space-based search sensitivity for V_{14} , V_8 , V_{16} , V_2 , V_{4+5} , and V_{12+13} , respectively. The space-based search sensitivity is shown with red dotted lines.

tometers that are insensitive to the pseudomagnetic signals to monitor the magnetic noise outside the μ -metal shield, which can then be actively compensated by the three-axis coils⁴⁵. Moreover, a multi-layer shield can be used to passively shield the remaining geomagnetic noise. Second, in addition to the noise of actual magnetic fields, the inertial rotation of nuclear-spin sensors caused by the vibration of space station, referred as gyroscopic effect, can produce an equivalent magnetic noise, which can not be suppressed by magnetic

shielding methods^{60,61}. This effect can be mitigated by utilizing fiber-optic gyroscopes with a superior rotation sensitivity. This allows for the subtraction of the influence caused by the measured rotational frequency. Third, cosmic radiation may introduce noise by falsely triggering signals and impair the semiconductor devices of space quantum sensors. One potential solution is to employ radiation-resistant chip and enclose integrated circuits and optical systems in shielding boxes.

Search sensitivity

The space-based search sensitivity for long-range spin-dependent interactions is estimated in this work. The proposed sensitivity is divided into two phases indicated by red dotted lines in Fig. 4 with the detection duration of 100 days. Here the phase 1 represents a conservative estimation based on spin sensors with the magnetic sensitivity of $100 \text{ fT/Hz}^{1/2}$, commonly achieved in terrestrial experiments. The phase 2 is based on the standard quantum limit of $0.01 \text{ fT/Hz}^{1/2}$ [56] and signifies the ultimate achievable sensitivity in space-based searches. Benefiting from macroscopic relative-velocity enhancements and particle abundance, the space-based search approach can significantly improve the search sensitivity in phase 1 compared to previous terrestrial experiments and proposals, as shown in Fig. 4. The constraints and sensitivities of these terrestrial works are depicted with blue solid and dotted lines in Fig. 4, including polarized geoelectrons experiment²⁹ and the proposed high-density SmCo₅ Source experiment¹⁶. Specifically, in the case of spin-spin interactions with a force range $\lambda > 10^6 \text{ m}$, our search sensitivity exceeds the previous terrestrial sensitivities by more than 7 orders of magnitude for f_{16} , 6 orders of magnitude for f_{14} , 6 orders of magnitude for f_8 , 4 orders of magnitude for f_2 [16,29]. In the case of spin-mass interactions, the limits for f_{12+13} are possible to improve by more than 2 orders of magnitude in the force range of $10^6 \text{ m} < \lambda < 10^{10} \text{ m}$ [27,30]. For f_{4+5} in the force range of $\lambda > 10^6 \text{ m}$, the limits are possible to improve by more than one order of magnitude^{27,30}. Furthermore, the search sensitivity can be further enhanced by 4 orders of magnitude in phase 2.

The studies of long-range spin-dependent interactions between particles A_1 and A_2 can indirectly search for ultralight new particles χ (Fig. 1), which can be candidates for dark matter particles. This indirect searches could cover a large mass range without further hypothesis that the ultralight new particles are dark matter or the necessity to scan over their mass. For examples, the coupling strengths f_{14} , f_{12+13} , and f_2 would link to the appropriate property of the ultralight new particles, i.e., the product of interaction coupling constants

$$f_{14} = \frac{4v_h^2 \text{Im}(C) \text{Re}(C) m_1 m_2}{\Lambda^4}, \quad (13)$$

$$f_{12+13} = \frac{4g_A g_V}{\hbar c}, \quad (14)$$

$$f_2 = -g_A g_A, \quad (15)$$

where $\text{Re}(C)$ ($\text{Im}(C)$) is the tensor (pseudotensor) interaction coupling constant between γ' bosons and standard-model particles, and g_V (g_A) is the vector (axial) interaction coupling constant between Z' bosons and standard-model particles. For example, based on our proposal sensitivity shown in Fig. 4f, the search sensitivity for f_{12+13}^{nN} in space-based searches is possible to set the constraint on $g_A^n g_V^N$ between neutrons and nucleons as $|g_A^n g_V^N / (\hbar c)| < 10^{-54}$ in the mass range $m_\chi \leq 10^{-13} \text{ eV}$. As a consequence, the studies of long-range spin-dependent interactions can provide a promising approach to searching for ultralight new particles.

Other applications and outlook

While the primary consideration concentrates on the searches for new particles via spin-dependent interactions, the scheme of space-based quantum sensing can also be extended to yield substantial enhancements in the searches of other models beyond the standard model, such as axion halo surrounding the Sun (commonly referred as the solar halo)⁴³. This improvement can be attributed to several key advantages, especially the high density of dark matter. The solar halo is formed due to the Sun's external gravitational force rather than its self-interactions³⁸⁻⁴⁰. The density of solar halo can be approximated by an exponential function described as follows: $\rho_* \simeq \rho_0 \exp(-2r/R_*)$, where r represents distance from the Sun, ρ_0 is overall density normalization, and the radius of solar halo $R_* \propto m_\phi^{-2}$, with m_ϕ being the mass of dark matter^{42,43}. In comparison to terrestrial spin sensors, the space quantum sensors offer the advantage of operating in much closer proximity to the Sun, enabling the detection of dark matter with greater density. For example, the Parker Solar Probe is capable of approaching the Sun at a distance less than 0.1 au [62], allowing space quantum sensors to detect dark matter with a density that is more than 7 orders of magnitude higher compared to that in terrestrial experiments in the case of $m_\phi \simeq 4 \times 10^{-14} \text{ eV}$ and $R_* \simeq 0.1 \text{ au}$.

We consider using nuclear spin sensors to search for the axion-nucleon linear coupling, which is different from the utilization of atomic clocks for detecting oscillations of fundamental constants in ref. [43]. The pseudomagnetic field of the linear coupling interaction can be described by the equation $\vec{B}_{\text{pseu}} = g_{\phi NN} \gamma_n^{-1} \left(\frac{m_\phi \vec{v}}{\hbar} + \frac{\hat{r}}{R_*} \right) \frac{\sqrt{2\rho_*}}{m_\phi} \sin(\vec{k} \cdot \vec{r} - \omega t)$, where $g_{\phi NN}$ is the axion-nucleon spin coupling constant, γ_n is the gyromagnetic ratio of nucleons, \vec{v} represents the relative velocity between spin sensors and the Sun, \vec{k} and ω denote the wavevectors and frequencies of axion field, respectively⁴⁴. It is worthwhile to note that in addition to large dark matter density, high relative velocity can also enhance the pseudomagnetic fields. When hypothesizing the spin sensors are equipped in Parker Solar Probe, our projected sensitivity for $g_{\phi NN}$, based on the sensitivity in the terrestrial proposal of solar halo⁴¹, is possible to surpass the astrophysical limits. For example, in the case of $m_\phi \simeq 4 \times 10^{-14} \text{ eV}$, our projected sensitivity exceeds the astrophysical limits by more than 4 orders of magnitude for $g_{\phi NN}$.

We present an opportunity to explore ultralight exotic particles in unexplored parameter space, inaccessible to terrestrial experiments, using space-based quantum sensors. It is feasible to construct a "space-ground integrated" network that combines space spin sensors and terrestrial spin sensors. The inclusion of space quantum sensors in this network enables the establishment of a long-baseline array for dark matter detection. Benefiting from the longer measurement baselines, the integrated network has the potential to exhibit higher spatial resolution when trying to study the structure of dark matter, particularly if a signal is present. The increased baseline allows for improved mapping and characterization of the distribution and properties of dark matter, which can provide valuable insights into its nature. Additionally, this detection net-

work can be utilized to perform wide-field coherent detection of various fluctuating dark matter models, including dark matter halo models and axion star models^{38–44}.

Data availability

The data that support the plots within this paper and other findings of this study are available from the corresponding author upon reasonable request.

Code availability

The code that generated the plots within this paper and other findings of this study are available from the corresponding author upon reasonable request.

References

- ¹Amsler, C. *et al.* Review of particle physics. *Phys. Rev. B* **667**, 1–6 (2008).
- ²Peccèi, R. D. & Quinn, H. R. CP conservation in the presence of pseudoparticles. *Phys. Rev. Lett.* **38**, 1440 (1977).
- ³Wilczek, F. Problem of strong P and T invariance in the presence of instantons. *Phys. Rev. Lett.* **40**, 279 (1978).
- ⁴An, H., Pospelov, M., Pradler, J. & Ritz, A. Direct detection constraints on dark photon dark matter. *Phys. Lett. B* **747**, 331–338 (2015).
- ⁵Dobrescu, B. A. Massless gauge bosons other than the photon. *Phys. Rev. Lett.* **94**, 151802 (2005).
- ⁶Ammar, R. *et al.* Search for the familon via $B^\pm \rightarrow \pi^\pm X^0$, $B^\pm \rightarrow K^\pm X^0$, and $B^0 \rightarrow K_s^0 X^0$ decays. *Phys. Rev. Lett.* **87**, 271801 (2001).
- ⁷Dearborn, D. S., Schramm, D. N. & Steigman, G. Astrophysical constraints on the couplings of axions, majorons, and familons. *Phys. Rev. Lett.* **56**, 26 (1986).
- ⁸Jiang, M., Su, H., Garçon, A., Peng, X. & Budker, D. Search for axion-like dark matter with spin-based amplifiers. *Nat. Phys.* **17**, 1402–1407 (2021).
- ⁹Duffy, L. D. & Van Bibber, K. Axions as dark matter particles. *New J. Phys.* **11**, 105008 (2009).
- ¹⁰Kim, J. E. & Carosi, G. Axions and the strong CP problem. *Rev. Mod. Phys.* **82**, 557 (2010).
- ¹¹Safronova, M. *et al.* Search for new physics with atoms and molecules. *Rev. Mod. Phys.* **90**, 025008 (2018).
- ¹²Moody, J. & Wilczek, F. New macroscopic forces? *Phys. Rev. D* **30**, 130 (1984).
- ¹³Dobrescu, B. A. & Mocioiu, I. Spin-dependent macroscopic forces from new particle exchange. *J. High Energy Phys.* **2006**, 005 (2006).
- ¹⁴Fadeev, P. *et al.* Revisiting spin-dependent forces mediated by new bosons: Potentials in the coordinate-space representation for macroscopic- and atomic-scale experiments. *Phys. Rev. A* **99**, 022113 (2019).
- ¹⁵Kim, Y. J., Chu, P.-H., Savukov, I. & Newman, S. Experimental limit on an exotic parity-odd spin- and velocity-dependent interaction using an optically polarized vapor. *Nat. Commun.* **10**, 1–7 (2019).
- ¹⁶Ji, W., Fu, C. & Gao, H. Searching for new spin-dependent interactions with SmCo₅ spin sources and a spin-exchange-relaxation-free comagnetometer. *Phys. Rev. D* **95**, 075014 (2017).
- ¹⁷Afach, S. *et al.* Search for topological defect dark matter with a global network of optical magnetometers. *Nat. Phys.* **17**, 1396–1401 (2021).
- ¹⁸Wang, Y. *et al.* Search for exotic parity-violation interactions with quantum spin amplifiers. *Sci. Adv.* **9**, eade0353 (2023).
- ¹⁹Wang, Y. *et al.* Limits on axions and axionlike particles within the axion window using a spin-based amplifier. *Phys. Rev. Lett.* **129**, 051801 (2022).
- ²⁰Su, H. *et al.* Search for exotic spin-dependent interactions with a spin-based amplifier. *Sci. Adv.* **7**, eabi9535 (2021).
- ²¹Chui, T. & Ni, W.-T. Experimental search for an anomalous spin-spin interaction between electrons. *Phys. Rev. Lett.* **71**, 3247 (1993).
- ²²Arvanitaki, A. & Geraci, A. A. Resonantly detecting axion-mediated forces with nuclear magnetic resonance. *Phys. Rev. Lett.* **113**, 161801 (2014).
- ²³Jiang, M. *et al.* Floquet spin amplification. *Phys. Rev. Lett.* **128**, 233201 (2022).
- ²⁴Jiang, M., Su, H., Wu, Z., Peng, X. & Budker, D. Floquet maser. *Sci. Adv.* **7**, eabe0719 (2021).
- ²⁵Xiong, F. *et al.* Searching spin-mass interaction using a diamagnetic levitated magnetic-resonance force sensor. *Phys. Rev. Research* **3**, 013205 (2021).
- ²⁶Terrano, W. & Romalis, M. Comagnetometer probes of dark matter and new physics. *Quantum Sci. Technol.* **7**, 014001 (2021).
- ²⁷Wu, L., Zhang, K., Peng, M., Gong, J. & Yan, H. New Limits on Exotic Spin-Dependent Interactions at Astronomical Distances. *Phys. Rev. Lett.* **131**, 091002 (2023).
- ²⁸Hunter, L., Gordon, J., Peck, S., Ang, D. & Lin, J.-F. Using the earth as a polarized electron source to search for long-range spin-spin interactions. *Science* **339**, 928–932 (2013).
- ²⁹Hunter, L. & Ang, D. Using geoelectrons to search for velocity-dependent spin-spin interactions. *Phys. Rev. Lett.* **112**, 091803 (2014).
- ³⁰Clayburn, N. B. & Hunter, L. R. Using Earth to search for long-range spin-velocity interactions. *Phys. Rev. D* **108**, L051701 (2023).
- ³¹Chen, L., Liu, J. & Zhu, K. Ultrasensitive optomechanical detection of an axion-mediated force based on a sharp peak emerging in probe absorption spectrum. *Opt. Commun.* **479**, 126422 (2021).
- ³²Liang, H. *et al.* New constraints on exotic spin-dependent interactions with an ensemble-nv-diamond magnetometer. *Natl. Sci. Rev.* **10**, nwac262 (2023).
- ³³Ritter, R. C., Goldblum, C. E., Ni, W.-T., Gillies, G. T. & Speake, C. C. Experimental test of equivalence principle with polarized masses. *Phys. Rev. D* **42**, 977 (1990).
- ³⁴Terrano, W., Adelberger, E., Lee, J. & Heckel, B. Short-range, spin-dependent interactions of electrons: A probe for exotic pseudo-goldstone bosons. *Phys. Rev. Lett.* **115**, 201801 (2015).
- ³⁵Ding, J. *et al.* Constraints on the velocity and spin dependent exotic interaction at the micrometer range. *Phys. Rev. Lett.* **124**, 161801 (2020).
- ³⁶Wineland, D., Bollinger, J., Heinzen, D., Itano, W. & Raizen, M. Search for anomalous spin-dependent forces using stored-ion spectroscopy. *Phys. Rev. Lett.* **67**, 1735 (1991).
- ³⁷Kotler, S., Ozeri, R. & Kimball, D. F. J. Constraints on exotic dipole-dipole couplings between electrons at the micrometer scale. *Phys. Rev. Lett.* **115**, 081801 (2015).
- ³⁸Veltmaat, J., Schwabe, B. & Niemeyer, J. C. Baryon-driven growth of solitonic cores in fuzzy dark matter halos. *Phys. Rev. D* **101**, 083518 (2020).
- ³⁹Anderson, N. B., Partenheimer, A. & Wisner, T. D. Direct detection signatures of a primordial Solar dark matter halo. Preprint at <https://arxiv.org/abs/2007.11016> (2020).
- ⁴⁰Braaten, E. & Zhang, H. Colloquium: The physics of axion stars. *Rev. Mod. Phys.* **91**, 041002 (2019).
- ⁴¹Banerjee, A. *et al.* Searching for earth/solar axion halos. *J. High Energy Phys.* **2020**, 1–26 (2020).
- ⁴²Banerjee, A., Budker, D., Eby, J., Kim, H. & Perez, G. Relaxion stars and their detection via atomic physics. *Commun. Phys.* **3**, 1 (2020).
- ⁴³Tsai, Y.-D., Eby, J. & Safronova, M. S. Direct detection of ultralight dark matter bound to the Sun with space quantum sensors. *Nat. Astron.* **7**, 113–121 (2023).
- ⁴⁴Afach, S. *et al.* What can a GNOME do? Search targets for the Global Network of Optical Magnetometers for Exotic physics searches. *Ann. Phys.* **2300083** (2023).
- ⁴⁵Liu, L. *et al.* In-orbit operation of an atomic clock based on laser-cooled ⁸⁷Rb atoms. *Nat. Commun.* **9**, 2760 (2018).
- ⁴⁶Bassi, A. *et al.* A way forward for fundamental physics in space. *npj Micrograv.* **8**, 49 (2022).
- ⁴⁷Gu, Y. The China Space Station: a new opportunity for space science. *Natl. Sci. Rev.* **9**, nwab219 (2022).
- ⁴⁸Gibney, E., Biever, C. & Castelvecchi, D. Dark-matter probe launches era of Chinese space science: Monkey King is first in a line of Chinese space missions focused on scientific discovery. *Nature* **528**, 443–445 (2015).
- ⁴⁹Abdo, A. A. *et al.* The Fermi gamma-ray space telescope discovers the pulsar in the young galactic supernova remnant CTA 1. *Science* **322**, 1218–1221 (2008).
- ⁵⁰Bergström, L., Bringmann, T., Cholis, I., Hooper, D. & Weniger, C. New limits on dark matter annihilation from alpha magnetic spectrometer cosmic ray positron data. *Phys. Rev. Lett.* **111**, 171101 (2013).
- ⁵¹Ji, W. *et al.* New experimental limits on exotic spin-spin-velocity-dependent interactions by using SmCo₅ spin sources. *Phys. Rev. Lett.* **121**, 261803 (2018).

- ⁵²The orbital parameters of the China Space Station. <http://www.cmse.gov.cn/gfgg/zgkjzgdcs/> (2022).
- ⁵³Maus, S. *et al.* The US/UK world magnetic model for 2010–2015 (2010).
- ⁵⁴Buffett, B. A. Earth's core and the geodynamo. *Science* **288**, 2007–2012 (2000).
- ⁵⁵Alfe, D. & Gillan, M. J. First-principles simulations of liquid Fe-S under Earth's core conditions. *Phys. Rev. B* **58**, 8248 (1998).
- ⁵⁶Kominis, I., Kornack, T., Allred, J. & Romalis, M. V. A subfemtotesla multichannel atomic magnetometer. *Nature* **422**, 596–599 (2003).
- ⁵⁷Venema, B., Majumder, P., Lamoreaux, S., Heckel, B. & Fortson, E. Search for a coupling of the earth's gravitational field to nuclear spins in atomic mercury. *Phys. Rev. Lett.* **68**, 135 (1992).
- ⁵⁸Feng, Y.-K., Ning, D.-H., Zhang, S.-B., Lu, Z.-T. & Sheng, D. Search for monopole-dipole interactions at the submillimeter range with a ¹²⁹Xe-¹³¹Xe-Rb comagnetometer. *Phys. Rev. Lett.* **128**, 231803 (2022).
- ⁵⁹Zhang, S.-B. *et al.* Search for spin-dependent gravitational interactions at earth range. *Phys. Rev. Lett.* **130**, 201401 (2023).
- ⁶⁰Kornack, T., Ghosh, R. & Romalis, M. V. Nuclear spin gyroscope based on an atomic comagnetometer. *Phys. Rev. Lett.* **95**, 230801 (2005).
- ⁶¹Han, B., Chen, Y., Zheng, S., Li, M. & Xie, J. Whirl mode suppression for AMB-rotor systems in control moment gyros considering significant gyroscopic effects. *IEEE Trans. Ind. Electron.* **68**, 4249–4258 (2020).
- ⁶²Kasper, J. *et al.* Parker solar probe enters the magnetically dominated solar corona. *Phys. Rev. Lett.* **127**, 255101 (2021).

Acknowledgments

We thank Lei Zhao, Zhe Cao, and Chengzhi Peng for valu-

able discussions. This work was supported by the Innovation Program for Quantum Science and Technology (Grant No. 2021ZD0303205), National Natural Science Foundation of China (Grants No. T2388102, No. 11661161018, No. 11927811, No. 12004371, No. 12150014, No. 12205296, No. 12274395, No. 123B2063, No. 122261160569), Youth Innovation Promotion Association (Grant No. 2023474), Chinese Academy of Sciences Magnetic Resonance Technology Alliance Research Instrument and Equipment Development/Functional Development (Grant No. 2022GZL003), and Frontier Scientific Research Program of Deep Space Exploration Laboratory (Grant No. 2022-QYKYJH-HXYF-013).

Author contributions

X.M.H., Y.H.W., X.K. performed the simulation, analyzed the simulation data, and wrote the manuscript. M.J., X.H.P., Z.G.Z., J.F.D. proposed the concept, devised the experimental protocols, and wrote the manuscript. H.S., Z.W., Q.L., W.Q.Z. performed the simulation data. Y.S., L.L. added theoretical discussions and edited the manuscript. All authors contributed with discussions and checking the manuscript.

Competing interests

The authors declare that they have no competing interests.